

Exciton-Enhanced Photoemission from Doped Solid Rare Gases*

Zohar Ophir, Baruch Raz, and Joshua Jortner

Department of Chemistry, Tel-Aviv University, Tel-Aviv, Israel

(Received 9 April 1974)

We report the observation of exciton-induced photoemission resulting from electronic energy transfer from "free" exciton levels to impurity states in solid Xe and Kr. A diffusion length of $l_0 \approx 75 \text{ \AA}$ for Wannier excitons in solid Xe was deduced, corresponding to a diffusion coefficient of $D = 0.5 \text{ cm}^2 \text{ sec}^{-1}$. The energy of the bottom of the conduction band is $V_0 = -0.46 \pm 0.1 \text{ eV}$ for Xe and $V_0 = -0.23 \pm 0.1 \text{ eV}$ for Kr.

The physical information available concerning exciton dynamics in simple insulators such as solid rare gases is rather meager. The vacuum-ultraviolet luminescence spectra of pure solid Ar, Kr, and Xe exhibit the emission from rare-gas diatomic molecules, which results from an efficient exciton-trapping process.¹ No emission could be detected from exciton states in these solids.^{2,3} Thus, from the exciton radiative lifetime $\tau_r \approx 10^{-9} \text{ sec}$, we infer that exciton trapping occurs within $\tau_0 < \tau_r/100 \approx 10^{-11} \text{ sec}$. Relevant information regarding exciton dynamics can be obtained from experimental studies of photoemission resulting from electronic energy transfer to impurity states in solid rare gases. The impurity energy gap E_G^i in these simple solids is $E_G^i = I_g^i + P_+^i + V_0$, where I_g^i is the impurity gas-phase ionization potential, P_+^i is the medium polarization energy by the impurity positive ion, and V_0 represents the energy of the matrix conduction band (relative to the vacuum level).⁴ The photoemission threshold from the impurity is $E_x^i = E_G^i - V_0$. The lowest Wannier exciton states of the matrix, characterized by the energy levels E_n ($n=1, 2, \dots$), can be located either above or below E_x^i . In the former case, i.e., $E_n > E_x^i$, one will observe direct photoemission from impurity states in the energy range $E_x^i \leq E \leq E_1$. In the latter case, when $E_1 \leq E_x^i$, one can expect photoemission due to energy transfer from free exciton states, E_n ($n \geq 1$), of the solid to the impurity. This Auger-type impurity ionization process can result only from the "collision" of a free exciton with the impurity. The electronic energy E_M of the trapped diatomic molecule¹⁻³ is too low, i.e., $E_M \leq E_x^i$, to induce impurity ionization. We have observed a dramatic enhancement of the photoemission yield of lightly doped solid rare gases (doping level $< 1\%$) when excited into the exciton manifold of the host crystal. Exciton-induced photoemission was reported twenty years ago in alkali halides containing F centers.⁵ The present

experiments on solid rare gases provide information regarding free-exciton dynamics on the time scale $\tau_0 \approx 1 \text{ psec}$,⁶ prior to exciton trapping.

The systems studied were C_6H_6/Xe ($E_G^i = 7.75 \text{ eV}$ ⁷ and $E_1 = 8.40 \text{ eV}$ ⁸), and Xe/Kr [$E_G^i = 10.4 \text{ eV}$ and $E_1(^3P_1) = 10.17 \text{ eV}$].⁹ Photoemission studies were carried out in the energy range 6–11.5 eV. The vacuum-ultraviolet light source consisted of a high-pressure (2–5 atm), high-intensity, gas pulsed discharge lamp.¹⁰ The light was passed through a 0.3-m Czerny-Turner monochromator employing a spectral resolution of 5 Å ($\sim 0.025 \text{ eV}$). The monochromator was separated from the sample chamber by a LiF window. The optical arrangement allowed for a simultaneous measurement of optical absorption and photoemission yield. The emitter electrode consisted of a 3-mm-wide gold strip evaporated on a LiF window. The collector electrode was a gold ring 15 mm in diameter, located 30 mm from the emitter. The signal was amplified in two stages and integrated by a boxcar integrator. A noise level of $5 \times 10^{-18} \text{ A}$ was achieved. The samples were prepared by deposition of a gaseous mixture on the emitter electrode mounted on a variable-temperature helium-flow cryostat at 30–40°K. The gaseous mixtures were prepared and handled in an ultrahigh-vacuum system previously pumped down to less than 10^{-9} Torr . The sample chamber was pumped by an ion pump and a cryogenic pump down to less than 10^{-9} Torr .

The curve of photoemission yield,¹¹ for pure Xe, Fig. 1, agrees with previous work.^{12,13} A square-root extrapolation of the yield versus energy (see Fig. 1) results in $E_x = 9.74 \pm 0.05 \text{ eV}$ which together with the spectroscopic value $E_G = 9.28 \pm 0.05 \text{ eV}$ results in $V_0 = -0.46 \pm 0.10 \text{ eV}$ for pure Xe. At energies lower than the threshold a structure is observed (photoemission yield $\sim 1\%$) at 1380 Å, which coincides with the E_2 exciton states of Xe. Several possible interpretations of this effect are as follows: (1) Impurity ioniza-

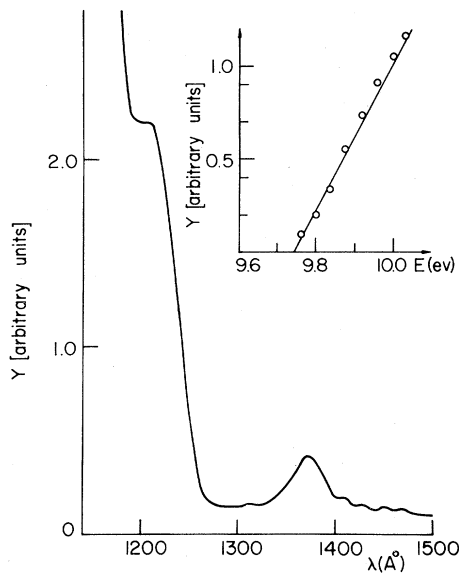


FIG. 1. Photoemission yield from solid Xe at 40°K. Upper inset: square-root extrapolation of the yield versus energy.

tion.¹² On the basis of our data for the C_6H_6/Xe we infer *inter alia* that the (unidentified) impurity concentration should exceed 5 ppm, which is rather high under our experimental conditions. (2) Nonlinear processes such as exciton-exciton collisions¹⁴ or exciton photoionization,¹⁴ which can be ruled out for the low light intensity employed in these experiments and in view of our observations that Y is independent of the light intensity. (3) Exciton diffusion to the gold substrate followed by electron ejection from the electrode. A preliminary result indicating that the 1380-Å photoemission peak decreases with increasing the sample thickness tends to support this mechanism.

In Fig. 2 we display the photoemission-yield curves for C_6H_6/Xe and for Xe/Kr . The emission onset for C_6H_6/Xe occurs at $E_x^i = 8.15 \pm 0.05$ eV which together with the spectroscopic value⁷ $E_G^i = 7.75$ eV results in $V_0 = -0.4 \pm 0.1$ eV for solid Xe in good agreement with the result for the pure solid. For Xe/Kr the onset $E_x^i = 10.68 \pm 0.1$ eV together with $E_G^i = 10.40$ eV results in $V_0 = -0.28 \pm 0.1$ eV for solid Kr.

The most prominent feature of these results involves the large photoemission yield in the energy range where light absorption occurs predominantly into the host-matrix exciton states below the photoemission threshold for the pure solids. The absolute quantum yields for photoemission

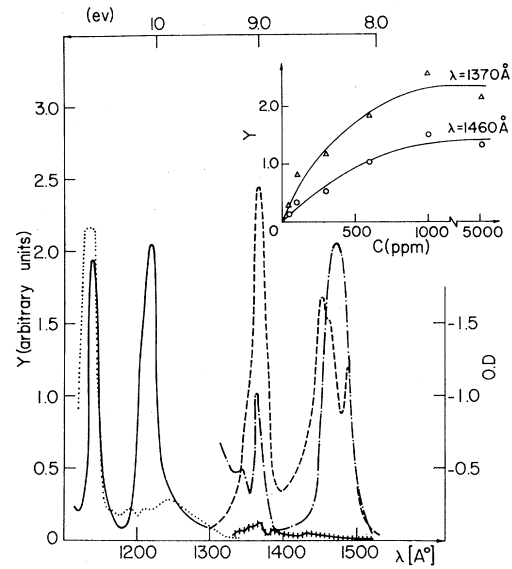


FIG. 2. Photoemission-yield curves from dilute (1%) impurity states in solid Xe and solid Kr measured at 30°K. Dashed curve, photoemission from benzene/Xe; dotted curve, photoemission from Xe/Kr. A photoemission-yield curve (hatched) for pure Xe is presented in the same arbitrary units as that for C_6H_6/Xe . The photoemission-yield curves are compared with the absorption spectra of pure Xe (dot-dashed curve) and of pure Kr (solid curve). Upper inset: the dependence of the photoemission yield on the benzene concentration C in C_6H_6/Xe solid films.

from C_6H_6/Xe are estimated¹⁵ to be approximately $Y \approx 20\%$ at 1455 Å and $Y \approx 30\%$ at 1380 Å. The photoemission originates from exciton-induced Auger-type impurity ionization.

The line shapes of the emission curves are expected to provide pertinent information regarding exciton dynamics. The C_6H_6/Xe system exhibits a minimum in the Y curve at 1480 Å which coincides with the maximum of the $n=1$ exciton state. The photoemission peaks at 1380 and 1350 Å practically coincide with the exciton energies E_2 (1380 Å) and E_3 (1345 Å). The dip in the photoemission curve at 1480 Å cannot be adequately explained in terms of the "dead-layer" theory,¹⁶ which results in $L \approx 150$ Å for the electron escape length and in the unphysically large value $h > 70$ Å for the width of the dead layer.

An attractive alternative approach to this problem involves a kinetic picture where competition between exciton trapping and energy transfer from excitons to homogeneously distributed impurities is considered. The number density $n(x, t)$ of "free" excitons at the distance x from the

surface is governed by the diffusion equation

$$\frac{\partial n(x,t)}{\partial t} = D \frac{\partial^2 n(x,t)}{\partial x^2} + kI_0 \exp(-kx) - \frac{n(x,t)}{\tau_0} - S[X]n(x,t), \quad (1)$$

where D is the exciton diffusion coefficient, k the absorption coefficient, I_0 the incident light intensity, S the rate constant for impurity ionization, and $[X]$ the impurity concentration. Under steady-state conditions, $n(x,t) = n(x)$, and Eq. (1) is readily solved using the appropriate boundary conditions $n(0) = n(\infty) = 0$. The photoemission quantum yield Y can be expressed in the form

$$Y = \frac{S[X]\tau}{1 - (kl)^2} \left[\frac{kL}{kL+1} - \frac{kl}{(l/L)+1} \right], \quad (2)$$

where the effective exciton lifetime is $\tau = (1/\tau_0 + S[X])^{-1}$ and $l = [D(1/\tau_0 + S[X])^{-1}]^{1/2}$ is the exciton diffusion length in the doped crystal, which is related to the diffusion length $l_0 = (D\tau_0)^{1/2}$ in the pure crystal via $l = l_0(1 + S\tau_0[X])^{-1/2}$.

In the limit $l = 0$, $Y \propto kL(kL+1)^{-1}$ and a monotonic increase of Y with k is exhibited. Thus our observation of the splitting of the Y curve about the $n=1$ exciton state implies that l is finite. Numerical calculations of $Y = Y(k)$ were performed utilizing the experimental absorption spectrum of solid Xe and employing a wide range of parameters $k_{\max}^{(1)}L$ and l/L . These calculations result in the following conclusions: (1) For $k_{\max}^{(1)}L > 2$ and $l/L > 0.03$ the Y curve around the $n=1$ exciton band exhibits a symmetric splitting revealing a minimum at E_1^{\max} . (2) The Y curve around the $n=2$ exciton band peaking at E_2^{\max} , which is characterized by a lower absorption coefficient $k_{\max}^{(2)} \approx 0.25k_{\max}^{(1)}$, is unsplit, its maximum coinciding with E_2^{\max} for $k_{\max}^{(1)}L < 8$. (3) The Y value at $E_{\max}^{(2)}$ and the maximum value of Y around $n=1$ are practically identical for the range of parameters mentioned in point (1). Our experimental results are in qualitative agreement with these features. The asymmetric splitting observed around E_1^{\max} results from the energy dependence of L about the threshold, while the ratio $Y(1370 \text{ \AA})/Y(1450 \text{ \AA}) \approx 1.5$ which is larger than the expected value of unity may originate from the inefficient electronic relaxation of the $n=2$ state to the $n=1$ state on the time scale of $\tau_0 \approx 10^{-12}$ sec, whereupon the parameters l_0 and L for the two electronic states may be somewhat different.

A semiquantitative fit of the Y line shape, the

concentration dependence of Y , and the absolute Y values was accomplished using Eq. (2) with the parameters $k_{\max}^{(1)}L = 2.5$, $l_0/L = 0.2$, and $S\tau_0 = 5 \times 10^{-19} \text{ cm}^{-3}$, all of which are reliable within a numerical factor of 2. The parameters l_0 and $S\tau_0$ for the $n=1$ excitons and for the $n=2$ excitons are identical within this margin of uncertainty. From $k_{\max}^{(1)} = 6 \times 10^5 \text{ cm}^{-1}$, we estimate a mean value of $L \approx 380 \text{ \AA}$, which is reasonable for solid rare gases at sufficiently high energies. The "free" exciton diffusion length is $l_0 \approx 75 \text{ \AA}$.

The diffusion length of excitons in solid Xe is lower than the corresponding values in organic crystals, i.e., $l_0 = 150 \text{ \AA}$ for singlet excitons¹⁷ ($\tau_0 = 25 \times 10^{-9}$ sec) and $l_0 = 10^5 \text{ \AA}$ for triplet excitons¹⁸ ($\tau_0 = 25 \times 10^{-3}$ sec) in crystalline anthracene. However, the exciton diffusion process in the solid rare gas occurs on an extremely short time scale, $\tau_0 \approx 10^{-12}$ sec, which implies that $D \approx 0.5 \text{ cm}^2 \text{ sec}^{-1}$ in this system. The rate constant $S \approx 5 \times 10^{-7} \text{ cm}^{-3} \text{ sec}^{-1}$ is consistent with this high D value. We now focus our attention on the interesting question of whether the excited motion is coherent or diffusive. Setting $S = \pi R^2 \langle V^2 \rangle^{1/2}$ and $D = \Lambda \langle V^2 \rangle^{1/2}$, where R is the reaction radius, $\langle V^2 \rangle^{1/2}$ the rms exciton group velocity, and Λ the exciton mean free path, we get $\Lambda = (D/S)\pi R^2$, which with $R = 10 \text{ \AA}$ results in $\Lambda \approx 3 \text{ \AA}$. Thus Λ is of the order of the lattice spacing and the exciton motion is diffusive (at least above $\sim 20^\circ \text{K}$).

Complementary information concerning dynamics of free excitons is obtained from optical line-shape studies.^{19,20} The Wannier exciton results in an $n=1$ exciton optical linewidth $\hbar\Gamma = 3.19 \times 10^{-4} m^{3/2} E_d^2$ (eV) for weak exciton-phonon coupling.¹⁹ Taking the experimental value $m = 0.5$ for the effective mass^{8,9} and $E_d = 1-3 \text{ eV}$ ^{20,21} for the deformation potential, we estimate $\hbar\Gamma \approx 10^{-4} - 10^{-3}$ eV which is appreciably lower than the experimental value $\hbar\Gamma = 0.075 \text{ eV}$ for the $n=1$ (3P_1) state. Thus the solid-rare-gas exciton states are close to the limit of strong exciton-phonon coupling which together with the low value of Λ provides *a posteriori* justification for the diffusion model adopted herein.

The photoemission yield of Xe/Kr (1% xenon), portrayed in Fig. 2, reveals that light absorption into the low-energy $n=1$ (3P_1) exciton state of solid Kr does not lead to impurity photoemission. The $n=1$ (1P_1) state of solid Kr is active in Auger-type energy transfer to the Xe impurity state. Thus the nonradiative $n=1$ (1P_1) \rightarrow $n=1$ (3P_1) multiphonon relaxation process in solid Kr is slow on the time scale of energy transfer from the mobile

"free" excitons to the Xe impurity.

*Work supported by the National Council for Research and Development, Israel.

¹J. Jortner, L. Meyer, S. A. Rice, and E. G. Wilson, *J. Chem. Phys.* **42**, 4250 (1965).

²A. Gedanken, B. Raz, and J. Jortner, *J. Chem. Phys.* **58**, 1178 (1973).

³O. Cheshnovsky, B. Raz, and J. Jortner, *J. Chem. Phys.* **59**, 3301 (1973).

⁴B. Raz and J. Jortner, *Proc. Roy. Soc., Ser. A* **317**, 113 (1970).

⁵L. Apker and E. Taft, *Phys. Rev.* **79**, 964 (1950), and **81**, 698 (1951).

⁶M. Martin, *J. Chem. Phys.* **54**, 3289 (1971).

⁷Gedanken, Raz, and Jortner, Ref. 2.

⁸G. Baldini, *Phys. Rev.* **128**, 1562 (1962).

⁹G. Baldini, *Phys. Rev.* **137**, A508 (1965).

¹⁰Z. Ophir, U. Even, B. Raz, and J. Jortner, "Pulsed High Pressure Lamp for the Vacuum Ultraviolet" (to

be published).

¹¹The photon current was normalized to the total photon flux hitting the sample. A small (10%) correction due to reflection of the pure matrix was neglected.

¹²J. F. O'Brien and K. J. Teegarden, *Phys. Rev. Lett.* **17**, 919 (1966).

¹³N. Schwentner, M. Skibowski, and W. Steinmann, to be published.

¹⁴S. I. Choi and S. A. Rice, *J. Chem. Phys.* **38**, 366 (1963).

¹⁵This estimate is based upon taking the absolute value $Y=13\%$ for solid Xe at 10.3 eV, obtained by Schwentner (private communication).

¹⁶M. Hebb, *Phys. Rev.* **81**, 702 (1951).

¹⁷O. Simpson, *Proc. Roy. Soc., Ser. A* **238**, 402 (1957).

¹⁸P. Avakian, V. Ern, R. E. Merrifield, and A. Suna, *Phys. Rev.* **165**, 974 (1968).

¹⁹Y. Toyozawa, *Progr. Theor. Phys.* **20**, 53 (1958).

²⁰A. Gold and R. S. Knox, *J. Chem. Phys.* **36**, 2805 (1962).

²¹S. D. Druger, *J. Chem. Phys.* **54**, 2339 (1971).

Temperature Dependence of Conductivity of Tetrathiafulvalene-Tetracyanoquinodimethane (TTF-TCNQ) Single Crystals

R. P. Groff, A. Suna, and R. E. Merrifield

Central Research Department, E. I. du Pont de Nemours and Company, Wilmington, Delaware 19898

(Received 22 May 1974)

The conductivity of single crystals of tetrathiafulvalene-tetracyanoquinodimethane (TTF-TCNQ) was measured over the temperature range 40–300 K. The maximum low-temperature conductivity parallel to the b axis ranged from 12–35 times the corresponding room-temperature value. The temperature dependence of the intrinsic conductivity (after residual resistivities were excluded) was the same for all crystals measured and was fitted by a $T^{-2.33 \pm 0.14}$ dependence for $60 \leq T \leq 300$ K.

Extraordinary maxima¹ in the apparent electrical conductivity of single crystals of tetrathiafulvalene-tetracyanoquinodimethane (TTF-TCNQ) have alternately been ascribed to the presence of superconducting fluctuations¹ or experimental artifacts.² There is considerable disagreement on the experimental results for the conductivity obtained in different laboratories.^{3,4} We have measured the conductivity along the a and b axes of a number of TTF-TCNQ single crystals. Our measurements show that the temperature dependence of the b -axis conductivity of TTF-TCNQ can be described by a single function, even for crystals whose conductivity enhancement differs by a factor of 3.

Solution-grown TTF-TCNQ crystals were prepared under argon, at room temperature, in acetonitrile, by diffusion of $5 \times 10^{-3}M$ solutions of the two components into an equal volume of

pure solvent. Both the TTF and TCNQ had been twice gradient sublimed under argon. Crystal growth was allowed to proceed for five days before harvesting. These crystals grow preferentially along the b axis with a laminar structure in which individual laminae are oriented parallel to the a - b plane. In order best to deal with the problem of nonuniform conductivity between laminae for b -axis measurements, crystals were selected with one perfectly developed a - b face and as free as possible from defects, inclusions, etc., visible in transmission microscopy with collimated incident light. Conventional dc measurement techniques were adopted with four silver-paste (Du Pont No. 7941 thinned with octyl acetate or hexyl acetate) electrodes attached to the best developed a - b face. This arrangement gave more reproducible results than such alternative electrode configurations as wrapping the